

# Native defects in hexagonal $\beta$ -Si<sub>3</sub>N<sub>4</sub> studied using density functional theory calculations

Maria-Elena Grillo\* and Simon D. Elliott

Tyndall National Institute, University College Cork, Lee Maltings, Cork, Ireland

Christoph Freysoldt

Max-Planck-Institute für Eisenforschung, D-40237 Düsseldorf, Germany

(Received 20 November 2010; revised manuscript received 9 January 2011; published 23 February 2011)

A comprehensive study of single native point defects in hexagonal silicon nitride ( $\beta$ -Si<sub>3</sub>N<sub>4</sub>) has been carried out based on density functional calculations of formation energies. Both nitrogen- and silicon-rich native defect centers form donor and acceptor states in the band gap of  $\beta$ -Si<sub>3</sub>N<sub>4</sub>, confirming their amphoteric behavior. Silicon dangling bonds resulting from structural nitrogen vacancies ( $V_N$ ) are the most abundant native defects, in particular, in their acceptor state ( $V_N^-$  and  $V_N^{3-}$ ). Hydrogenation promotes the appearance of Si dangling bond defects in the neutral state consistent with the observation of paramagnetic centers in the gap of amorphous silicon nitrides by electron spin resonance. This explains the utility of silicon nitride as charge trapping layer in nonvolatile memories.

DOI: 10.1103/PhysRevB.83.085208

PACS number(s): 71.55.Ht

## I. INTRODUCTION

Localization of electrons ( $e^-$ ) and holes ( $h^+$ ) by deep states (traps) in the band gap leads to the capability of silicon nitride films to function as long-term charge trapping layers in new generations of nonvolatile memory devices.<sup>1</sup> These traps have been attributed to different types of silicon dangling bonds, termed  $K$ -center defects, based on electron spin resonance (ESR) measurements,<sup>1-4</sup> and electronic structure calculations of some native defects.<sup>5-8</sup> However, a comprehensive characterization of the atomic and electronic structure of  $e^-$  and  $h^+$  traps in silicon nitride is still missing. Yet, in order to optimize the efficiency of silicon nitrides for application in nonvolatile memories, it is crucial to understand the charge trapping mechanism of the intrinsic defects.

We have addressed this issue by a first-principles study of all native point defects in hexagonal  $\beta$ -Si<sub>3</sub>N<sub>4</sub>. The present calculations quantitatively identify the  $K$ -center defects responsible for the memory traps as Si-Si bonds arising after significant atomic rearrangements at unsaturated Si dangling bonds, in particular, on nitrogen vacancies ( $V_N$ ) in the structure, on interstitial Si atoms ( $Si_i$ ), and on silicon antisites ( $Si_N$ ). All Si-rich defects are able to trap both  $e^-$  and  $h^+$  simultaneously, consistent with the weak electron spin resonance (ESR) signal corresponding to observable neutral  $K^0$  centers. Hence, Si dangling bonds exist as diamagnetic charged  $K^+$  and  $K^-$  centers, as originally proposed by ESR studies in amorphous silicon nitride ( $a$ -SiN<sub>x</sub>:H) films.<sup>1-3</sup> Nonetheless, the non-negligible concentration of paramagnetic  $K^0$  centers in  $a$ -SiN<sub>x</sub>:H of 10–20 % observed by ESR<sup>9</sup> can only be explained when hydrogenation of silicon dangling bonds at Si-rich defects is considered. The present study demonstrates that hydrogenation of unsaturated silicon sites at nitrogen vacancies ( $V_NH$ ) and at antisites ( $Si_NH$ ) in the lattice favors the neutral state of Si-rich defect centers against diamagnetic charged states within a certain Fermi energy range in the gap. This result is consistent with the observed formation of metastable  $K^0$  centers by ultraviolet (UV) illumination, and subsequent charging upon gentle annealing (200 °C).<sup>9,10</sup> This recombination process ( $2K^0 \rightarrow K^+ + K^-$ ), which is

characteristic of amphoteric defects with associated negative effective correlation energy ( $U_c$ ), has long been proposed to interpret the ESR and charge measurements.<sup>1-3,9</sup> Comparing the formation energies of all intrinsic single point defects in  $\beta$ -Si<sub>3</sub>N<sub>4</sub>, the present calculations show that electron-acceptor Si dangling bonds in particular at nitrogen vacancies (termed  $V_N$  in Fig. 1) are the main source of charge traps in Si enriched samples. This finding confirms the interpretation of low-temperature ESR data<sup>4</sup> suggesting an *excess* of negatively charged defect centers in  $a$ -SiN<sub>x</sub>:H as the main source of charge traps.

## II. METHOD

The most stable charged state of a defect is determined by calculating the formation energy as a function of the Fermi energy (i.e., chemical potential of the electrons).<sup>11</sup> The formation energy of a defect in charged state  $q$  is obtained as

$$E^f(q) = E^{\text{tot}}(q) - n_{\text{Si}}\mu_{\text{Si}} - n_{\text{N}}\mu_{\text{N}} - qE_{\text{F}},$$

where  $E^{\text{tot}}(q)$  is the total energy of the defect as calculated for a relaxed supercell model,  $n_{\text{Si}}$  and  $n_{\text{N}}$  are the number of silicon and nitrogen atoms in the supercell, respectively,  $\mu_{\text{Si}}$  and  $\mu_{\text{N}}$  are their chemical potentials, and  $E_{\text{F}}$  is the Fermi energy. A low formation energy indicates a high equilibrium concentration of the corresponding defect, whereas a high value implies that it does not occur spontaneously upon processing. Therefore, the formation energy depends on the growth condition through the chemical potentials defining a reservoir of Si and N, and on the electronic reservoir or Fermi level. The range of chemical potentials is constrained by the equilibrium with bulk  $\beta$ -Si<sub>3</sub>N<sub>4</sub>. Therefore, the minimum  $\mu_{\text{N}} = \frac{1}{4}(\mu_{\text{Si}_3\text{N}_4} - 3\mu_{\text{Si}})$  is that corresponding to the maximum  $\mu_{\text{Si}}$  at which bulk silicon segregates. The electrical behavior of the defect is defined by the electronic transition level  $\epsilon(q/q')$ . The transition energy  $\epsilon(q/q')$  is the Fermi energy value above which the charge state  $q$  changes to a more stable  $q'$  state. The charge transition energy allows to characterize the localized defect levels (trap

states) in terms of their energy depth within the band gap (i.e., shallow vs deep).

The problem of calculating charged defect states is approached by embedding the defect in a periodic supercell with a neutralizing background. This approach has been successfully used for large supercells and low charged states.<sup>11</sup> However in the present study the formation energies for the nitrogen vacancy in the  $q = -3$  charged state were corrected to account for the artificial electrostatic interactions introduced by the periodic supercell approximation. This has been done using a recent correction scheme which explicitly calculates the artificial electrostatic interactions between defects of neighboring cells, and that of the background charge with the defect within the reference supercell.<sup>18</sup> A theoretical value for the dielectric constant of 8.514 for the  $\beta$ - $\text{Si}_3\text{N}_4$  supercell at the GGA-PBE level<sup>19</sup> was used to calculate the electrostatic potential corrections.

### A. Bulk structure and supercell calculations

Formation energies for native defects in bulk silicon nitride ( $\beta$ - $\text{Si}_3\text{N}_4$ ) were calculated using density functional theory (DFT) within the generalized gradient approximation of Perdew, Burke, and Ernzerhof (GGA)<sup>12</sup> and the all-electron projector-augmented wave method (PAW)<sup>13</sup> as implemented in the VASP package.<sup>14</sup> The hexagonal primitive cell of  $\beta$ - $\text{Si}_3\text{N}_4$  with space group  $P6_3m$  has been optimized with respect to the crystallographic lattice parameters and to the four inner parameters of the coordinates of the 14 atoms (six Si and eight N) per unit cell. The structure comprises a three-dimensional network of distorted  $\text{SiN}_4$  tetrahedra bonded to each other along the  $c$  axis of the hexagonal unit cell. The N are threefold coordinated by silicon atoms of which two atoms are in a planar configuration (Si-N bond type 1 in Table I) occupying special fixed positions. The calculated Si-N bond lengths and inner coordinates are listed in Table I compared to the experimental structure, and to previous DFT results obtained at the local-density level of approximation (LDA).<sup>15</sup> The bulk modulus was obtained by fitting the GGA-PBE total energy  $E(V)$  vs volume ( $V$ ) to the Vinet equation of state. The lattice parameters ( $a = 7.562 \text{ \AA}$  and  $c/a = 0.383$ ) and bulk modulus (263 GPa) thereby obtained are consistent with the experimental values<sup>16</sup> of 7.608  $\text{\AA}$ , 0.380 and 256 GPa, respectively. A band energy gap of 4.2 eV was obtained compared to the reported experimental range<sup>17</sup> of 4.5 to 5.5 eV depending on the SiN stoichiometry. Single-point isolated

TABLE I. Calculated (GGA-PAW) Si-N bond lengths ( $\text{\AA}$ ) and inner coordinates in  $\beta$ - $\text{Si}_3\text{N}_4$ . The bond lengths are compared to previous LDA results.<sup>15</sup> Percentage deviations from the corresponding experimental<sup>16</sup> (Exp.) values are given for the GGA-PAW theoretical data.

Si-N bond	Exp.	GGA-PAW	LDA
1	1.745	1.744 (-0.1%)	1.719
2	1.739	1.750 (+0.6%)	1.726
3	1.729	1.749 (+1.2%)	1.728
Si	(0.1733, 0.7694, $\frac{1}{4}$ )	(0.1753, 0.7692, $\frac{1}{4}$ )	
N	(0.3323, 0.0314, $\frac{1}{4}$ )	(0.3300, 0.0312, $\frac{1}{4}$ )	

defects were modeled using a 280-atom supercell obtained by  $(2 \times 2 \times 5)$  translations of the primitive unit cell of  $\beta$ - $\text{Si}_3\text{N}_4$ , assuring similar distances of 18 to 19  $\text{\AA}$  between defects from neighboring cells along different directions. For the total energy calculations of native defects with and without hydrogen we used a kinetic energy cutoff of 400 eV for the plane-wave basis set, and a grid of  $(2 \times 2 \times 2)$  special points for Brillouin zone integrations.

## III. NATIVE POINT DEFECTS

The lowest formation energies for all native single point defects calculated considering Si rich conditions are shown in Fig. 1 spanning an energy gap of 5.0 eV. The changes in slope in Fig. 1 correspond to changes in the lowest energy charged state within the energy gap (i.e., thermodynamic transition energies). At all energies, nitrogen vacancies are found to be the most favorable native defects. The facile formation of the nitrogen vacancies indicates that they might play a role in donor compensation (counteracting the prevailing conductivity), and explains the large amounts of microvoids observed in silicon nitride thin films.

### A. Nitrogen vacancies

The nitrogen vacancy exhibits a  $(1 + /1-)$  transition at 1.8 eV above the calculated valence band (VB) edge. The  $q = -1$  charged state exhibits a doubly occupied level in the gap as also found by previous theoretical studies.<sup>20</sup> The neutral  $V_N^0$  is not stable within the band gap, confirming the negative effective correlation  $U_c$  (amphoteric character) of this defect discussed at length in the literature.<sup>1-3,9</sup> The energy position of the transition  $(1 + /1-)$  level is in agreement with previous electronic structure calculations of the  $N_3 = \text{Si}$  dangling bond level in the gap.<sup>5,6</sup> Moreover, this defect level has been observed by optical absorption spectroscopy<sup>21</sup> for all silicon nitride compositions. Despite correcting the formation energy of the  $q = -3$  charged state for spurious (attractive) electrostatic interactions intrinsic to supercell calculations,<sup>18</sup> it is the most stable charged state at high Fermi energy values

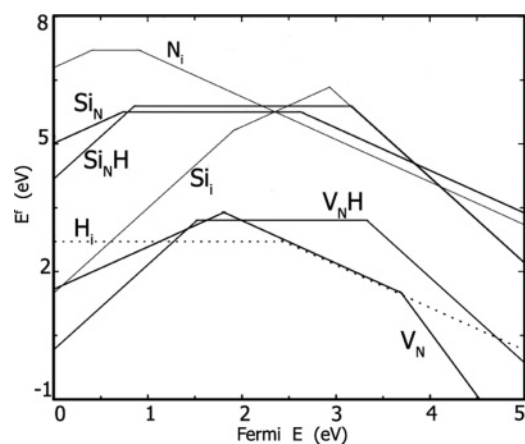


FIG. 1. Defect formation energies  $[E^f(q)]$  as a function of the Fermi level ( $E_F$ ) for native defects in  $\beta$ - $\text{Si}_3\text{N}_4$ .  $E^f(q)$  calculated with respect to the VB edge ( $E_F = 0 \text{ eV}$ ) are shown in an energy range spanning a band gap of 5 eV.

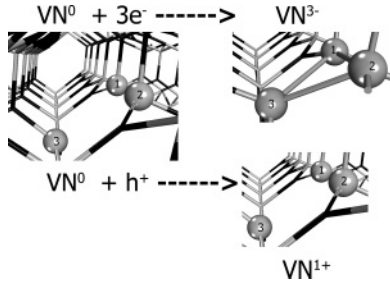


FIG. 2. Structural models for a nitrogen vacancy in the neutral state ( $q = 0$ ), in the positive ( $q = +1$ ) and highest negative charge state ( $q = -3$ ) below the CB (right). The host structure is shown in a stick representation. The Si atoms around the N vacancy are shown as light grey balls.

below the conduction band (CB), see Fig. 1. We have also considered the spin-polarized  $q = -2$  charged state. However, the calculated formation energies show that it is never stable in the gap compared to the  $q = -1$  (doubly occupied) and  $q = -3$  charged states.

For the ionized  $q = +1$  charged state, the calculations show contraction of, in particular,  $\text{Si}_3$ -N bonds around the N vacancy (Fig. 2 and Table II). We suggest that this is due to increased hybridization of the Si-dangling bonds to the remaining N atoms in the distorted  $\text{SiN}_3$  tetrahedra. The stability of the  $-3$  charged state arises from a large relaxation of the neighboring Si atoms which move by up to 12% of the equilibrium bond length. In this charge state, Si atoms relax around the N vacancy, forming Si-Si bonds (bond lengths about 2.5 Å) and increasing Si-N bond lengths to neighboring N atoms (Table II and Fig. 2). As a consequence of the obtained large outward relaxations for the  $-3$  charged structure, rehybridization among those Si atoms lowers the energy of Si dangling bond states originally in the CB<sup>22</sup> shifting them into the band gap at about 1 eV below the CB edge. This is characteristic of a negative- $U_c$  impurity, which is associated with outstanding lattice relaxations of one particular charged state.<sup>11</sup>

Large amounts of hydrogen are present in silicon nitride sample production.<sup>7,8</sup> The role of hydrogen in the formation of local point defects in hydrogenated films  $\alpha$ - $\text{Si}_3\text{N}_4$ :H was considered by calculating all possible H-saturated Si-rich defects. The chemical potential of hydrogen in the gas phase ( $\mu_{\text{H}}$ ) thereby used was calculated using statistical thermody-

TABLE II. Calculated bond lengths (Å) for the nitrogen vacancy in the neutral state ( $q = 0$ ), in the positive ( $q = +1$ ) and negative charge state ( $q = -3$ ). Deviations from the corresponding *ab initio* bulk values are given in brackets.

	$q = +1$	$q = 0$	$q = -3$
$\text{Si}_{1,2}$ -N	1.749(0.0%)	1.763(+ 1.1%)	1.904(+ 8.8%)
	1.731(-0.7%)	1.740(-0.6%)	1.864(+ 6.9%)
	1.737(-0.7%)	1.777(+ 1.6%)	1.864(+ 6.9%)
$\text{Si}_3$ -N	1.714(-1.7%)	1.793(+ 2.4%)	1.831(+ 5.0%)
	1.720(-1.7%)	1.793(+ 2.4%)	1.962(+ 12.1%)
	1.720(-1.7%)	1.777(+ 1.9%)	1.962(+ 12.1%)
$\text{Si}_1$ - $\text{Si}_2$			2.489
$\text{Si}_{1,2}$ - $\text{Si}_3$			2.511

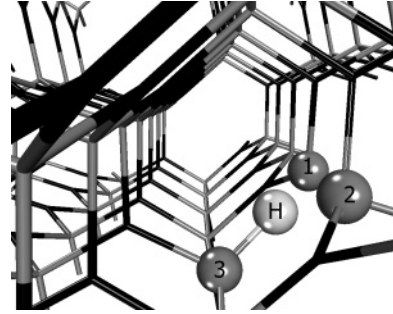


FIG. 3. Structural model for the H-saturated nitrogen vacancy in the neutral state. The host structure is shown in a stick representation. The Si and H atoms around the N vacancy are shown in light grey and white balls, respectively.

namics for a realistic external  $\text{H}_2$  partial pressure of 0.1 bar as a function of temperature. The choice of  $\mu_{\text{H}}$  is consistent with the abundance of hydrogen during film preparation originated from the dissociation of the ammonia precursor ( $\text{NH}_3$ ) molecules in the common preparation processes.

Upon hydrogenation the lowest energy charge transition level for nitrogen vacancies (termed  $\text{V}_{\text{N}}\text{H}$  in Fig. 1) corresponds to a  $(2 + /0)$  transition at 1.5 eV above the VB maximum. The neutral state then remains stable in the gap up to about 2 eV above VB edge. This is consistent with the ultraviolet induced observation of paramagnetic  $K^0$  centers by ESR experiments.<sup>9</sup> Nonetheless for increasing Fermi energies up to the CB edge the lowest energy charge transition is the  $(1 - /3-)$  level at 3.7 eV (Fig. 1) above the VB edge of the *unsaturated* Si dangling bonds on N vacancies. This result is at odds with the predictions made by previous DFT studies,<sup>7,8,20</sup> which proposed hydrogenated Si dangling bond as the main source for memory traps in silicon nitride memories. None of these studies, however, calculated relative Si-rich defect formation energies that allow relative defect concentrations to be assessed. In addition, we note that particularly large supercells are required to obtain the breathing reconstruction responsible for the  $q = -3$  charged state. The calculated H-saturated nitrogen vacancy structure is displayed in Fig. 3. As expected, hydrogen binds onto the  $\text{Si}_3$  type sites (Si-H = 1.413 Å) which were found to have the largest Si-N bond elongation in the the neutral and in the most abundant  $q = -3$  charged state, see Table II. The neutral hydrogen interstitial is preferred within a Fermi energy range below the midgap. The stability of  $\text{H}^-$  for  $E_{\text{F}}$  values close to the CB indicates the tendency of hydrogen to compensate the prevailing conductivity, as previously observed in amorphous  $\alpha$ -Si:H and in GaN.<sup>23</sup>

## B. Silicon antisites

Saturation of silicon antisites ( $\text{Si}_{\text{N}}\text{H}$  in Fig. 1) with hydrogen lowers the formation energy of charged states. With increasing Fermi energy, a charge transition  $(2 + /0)$  at 0.9 eV above the VB for the H-saturated  $\text{Si}_{\text{N}}\text{H}$  form is obtained. The neutral (paramagnetic) form of the unsaturated antisite,  $\text{Si}_{\text{N}}^0$ , becomes visible to ESR up to about the midgap. At high  $E_{\text{F}}$  below the CB, the  $q = -2$  charged state of the hydrogenated form  $\text{Si}_{\text{N}}\text{H}$  is the lowest energy defect with a transition level

(0/2<sup>-</sup>) at 3.2 eV with respect to the VB maximum. It is stabilized by a large outward breathing relaxation into the large 12-member ring cage similar to the interstitial Si. The silicon interstitial ( $\text{Si}_i$ ) induces deep electron and hole traps, as seen in Fig. 1, where the lowest energy charged states are the doubly negative and positive charged states, respectively. The neutral state is not stable in the gap, proving its amphoteric character. Hydrogen does not bind on interstitial silicon. Unsaturated interstitial Si atoms are stabilized through coordination to host Si and N atoms.

### C. Nitrogen interstitials

Nitrogen dangling bond defect centers were also studied by introducing interstitial nitrogen atoms in the lattice ( $\text{N}_i$ ). This defect was first identified by Warren *et al.*<sup>24</sup> by ESR measurements. Nitrogen-dangling bonds can trap both electrons and holes, see Fig. 1. The acceptor state ( $\text{N}_i^-$ ) is the most stable in almost the entire range of Fermi energies in the gap. The occurrence of  $\text{N}_i^-$  was observed by Warren *et al.*<sup>25</sup> for low temperature ( $-163^\circ\text{C}$ ) illumination of N-rich silicon nitrides, and confirmed by electronic structure calculations.<sup>6</sup> The donor  $\text{N}_i^+$  formation will be very unlikely. The relatively high formation energies calculated for N-dangling bonds are consistent with their observed metastability.<sup>24</sup>

## IV. SI-SI DEFECTS AND CHARGE TRAPS IN SILICON NITRIDE

The electron-acceptor levels in the gap introduced by nitrogen vacancies ( $\text{V}_\text{N}$ ) are relevant to interpret the recently reported peak in the trap energy spectrum of a silicon nitride based nonvolatile memory stack,<sup>26</sup> as shown schematically in Fig. 4. In this work, trap spectroscopy by charge injection and sensing (TSCIS) was used to scan for acceptor traps in the topmost 2 eV of the silicon nitride band gap. As seen in the TSCIS measurement principle illustrated in Fig. 4(b), electrons are injected through the  $\text{SiO}_2$  film into the band gap of silicon nitride during device programming.<sup>27</sup> Additionally, the recapture of Poole-Frenkel emitted electrons from the CB is detected by TSCIS.<sup>27</sup> For stoichiometric and Si-rich silicon nitride, peaks in trap density were found at 1.6 eV and 1.4 eV below the CB edge, respectively.<sup>26</sup> Our results (Fig. 1) show that the most stable defect at energies below the CB edge is the N vacancy, which is an acceptor, with a calculated electronic transition level from the charged states  $q = -1$  to  $q = -3$  at 3.7 eV above the VB edge. This corresponds to 1.3 eV below the CB edge, and is therefore consistent with the trap density spectrum measured by TSCIS. Although, the GGA-PBE exchange used cannot provide quantitative accuracy for the calculated defect energy levels, the obtained N-vacancy defects provide a consistent interpretation of the observed trap density spectrum. Hence, the present investigation unravels apparent contradictions in previous theoretical studies regarding the

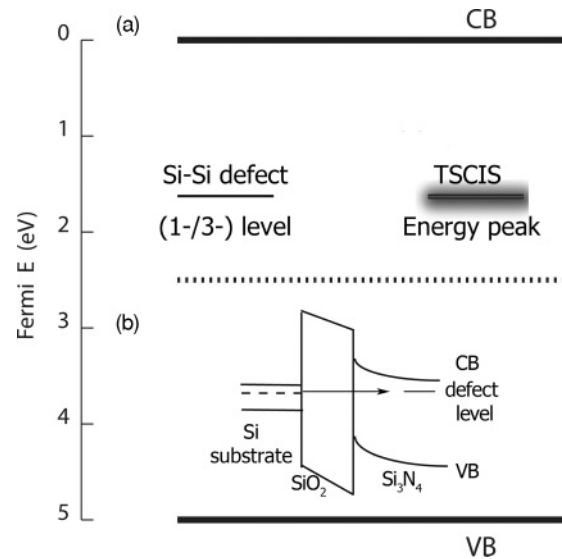


FIG. 4. Schematic representation of the energy position in the band gap of  $\beta\text{-Si}_3\text{N}_4$  of the calculated transition level (1-/3-) introduced by N vacancies and reported peak of the TSCIS trap energy spectrum (a).<sup>26</sup> Measurement principle of trap energy levels by TSCIS<sup>27</sup> (b).

atomic structure of electron and hole traps in silicon nitride films.

## V. CONCLUSIONS

To summarize, the present study demonstrates that native point defect centers in  $\beta\text{-Si}_3\text{N}_4$  show acceptor and donor type states in the gap, simultaneously, consistent with the observed weak paramagnetic signals observed by ESR corresponding to the neutral state. Hence, upon charge injection both types of free carriers ( $\text{h}^+$  and  $\text{e}^-$ ) are captured by negatively and positively charged states in the gap, respectively. Silicon dangling bonds around nitrogen vacancies are the thermodynamically preferred native defects, and acceptor type states of these defects are more easily formed (i.e., higher concentration). Hydrogenated Si antisites ( $\text{Si}_\text{N}\text{H}$ ) also show acceptor states with a fairly high solubility in the lattice as compared to other possible charged states. These results indicate that in Si-enriched silicon nitride there will be an excess of acceptor levels serving as charge traps upon charge injection in nonvolatile memory devices. This explains the behavior that has already been found in ESR experiments.<sup>1-4</sup>

## ACKNOWLEDGMENTS

This work has been funded by the EU through the GOSSAMER project (214431). M.E.G. gratefully acknowledges Catherine Stampfl for her assistance and benefited from critical discussions with Gianfranco Pacchioni and Jörg Neugebauer.

\*Current address: Lauterer Str. 17A, D-81545 München, Germany; megrillo@gmx.net

<sup>1</sup>D. T. Krick, P. M. Lenahan, and J. Kanicki, *J. Appl. Phys.* **64**, 3558 (1988).

<sup>2</sup>S. Fujita and S. Sasaki, *J. Electrochem. Soc.* **132**, 398 (1985).

<sup>3</sup>P. M. Lenahan and S. E. Curry, *Appl. Phys. Lett.* **56**, 157 (1990).

<sup>4</sup>Y. Kamigaki, S.-I. Minami, and H. Kato, *J. Appl. Phys.* **68**, 2211 (1990).



- <sup>5</sup>J. Robertson and M. J. Powell, *Appl. Phys. Lett.* **44**, 415 (1984).
- <sup>6</sup>G. Pacchioni and D. Erbetta, *Phys. Rev. B* **61**, 15005 (2000).
- <sup>7</sup>M. Petersen and J. Roizin, *Appl. Phys. Lett.* **89**, 053511 (2006).
- <sup>8</sup>V. A. Gritsenko, S. S. Nekrashevich, V. V. Vasilev, and A. V. Shaposhnikov, *Microelectron. Eng.* **86**, 1866 (2009).
- <sup>9</sup>W. L. Warren, J. Kanicki, and E. H. Poindexter, *Colloids Surf. A* **115**, 311 (1996).
- <sup>10</sup>F. D. Tober, J. Kanicki, and M. S. Crowder, *Appl. Phys. Lett.* **59**, 1723 (1991).
- <sup>11</sup>C. G. Van de Walle and J. Neugebauer, *J. Appl. Phys.* **95**, 3851 (2004).
- <sup>12</sup>J. P. Perdew, K. Burke, and M. Ernzerhof, *Phys. Rev. Lett.* **77**, 3865 (1996).
- <sup>13</sup>P. E. Blöchl, *Phys. Rev. B* **50**, 17953 (1994).
- <sup>14</sup>G. Kresse and J. Furthmüller, *Comput. Mater. Sci.* **6**, 15 (1996); *Phys. Rev. B* **54**, 11169 (1996).
- <sup>15</sup>R. Belkada, T. Shibayanagi, M. Naka, and M. Kohyama, *J. Am. Ceram. Soc.* **83**, 2449 (2000).
- <sup>16</sup>P. Villars, *Crystallographic Data for Intermetallic Phases* (ASM International, Materials Park, 1997), Vol. 2.
- <sup>17</sup>A. V. Vishnyakov, Yu. N. Novikov, V. A. Gritsenko, and K. A. Nasyrov, *Solid-State Electron.* **53**, 251 (2009); R. Kärcher, L. Ley, R. L. Johnson, *Phys. Rev. B* **30**, 1896 (1984).
- <sup>18</sup>C. Freysoldt, J. Neugebauer, and C. G. Van de Walle, *Phys. Rev. Lett.* **102**, 016402 (2009).
- <sup>19</sup>S. Baroni and R. Resta, *Phys. Rev. B* **33**, 7017 (1986).
- <sup>20</sup>E. Vianello, E. Nowak, L. Perniola, F. Driussi, P. Blaise, G. Molas, B. De Salvo, and L. Selmi, Proceedings of the International Memory Workshop, 2010, Seoul, Institute of Electrical and Electronics Engineers (IEEE) Curran Associates Inc., p. 106.
- <sup>21</sup>J. Kanicki, W. L. Warren, C. H. Sieger, and P. M. Lenahan, *J. Non-Cryst. Solids* **137-138**, 291 (1991).
- <sup>22</sup>Y.-N. Xu and W. Y. Ching, *Phys. Rev. B* **51**, 17379 (1995).
- <sup>23</sup>C. G. Van de Walle and J. Neugebauer, *Nature (London)* **423**, 626 (2003).
- <sup>24</sup>W. L. Warren, P. M. Lenahan, and S. E. Curry, *Phys. Rev. Lett.* **65**, 207 (1990).
- <sup>25</sup>W. L. Warren, J. Robertson, and J. Kanicki, *Appl. Phys. Lett.* **63**, 2685 (1993).
- <sup>26</sup>A. Suhane, A. Arregghini, R. Degraeve, G. Van den Bosch, L. Breuil, M. B. Zahid, M. Jurczak, K. De Meyer, and J. Van Houdt, *IEEE Electron Device Lett.* **31**, 77 (2010).
- <sup>27</sup>R. Degraeve, M. Cho, B. Govoreanu, B. Kaczer, M. B. Zahid, J. Van Houdt, M. Jurczak, and G. Groeseneken, Proceedings of the International Conference on Consumer Electronics, 2008, Las Vegas, Institute of Electrical and Electronics Engineers (IEEE) Curran Associates Inc., p. 775.